

The Bounded System of N Equal-Mass Distinguishable Hard Particles

BIN KANG CHENG

Departamento de Física, Universidade Federal do Paraná, Curitiba, Brasil

Recebido em 8 de Junho de 1979

We investigate the dynamical behavior of the system of N equal-mass distinguishable hard particles confined in a one-dimensional box of length R . The collisions among the particles and the collisions between the particle and the wall are assumed to be elastic. By introducing "Mirror-Image" transformation and by using distinguishability of the particles, we are able to obtain the analytical solution in Newtonian sense. We then study the possible ordering of different collisions for $N = 2$ case. Finally, the equilibrium distribution function has been derived and from which some statistical quantities have been calculated.

Investigamos o comportamento dinâmico do sistema de N partículas duras, distinguíveis, de mesma massa, dentro de uma caixa unidimensional de comprimento R . As colisões entre as partículas e as colisões entre partícula e parede são supostas elásticas. Introduzindo a transformação "Espelho-Imagem" e usando a distinguibilidade das partículas, nos é possível obter a solução analítica Newtoniana. Estudamos então as ordens possíveis das colisões diferentes para o caso $N = 2$. Finalmente, a função distribuição de equilíbrio é deduzida e algumas quantidades estatísticas são calculadas através desta.

1. INTRODUCTION

In ergodic theory¹, we are interested in the qualitative behavior of classically mechanical systems and of simple physical systems (models), which may throw light on some fundamental problems such as

irreversibility in statistical mechanics. However, it is well known that no indication of how systems approach equilibrium can be obtained in ergodic theory. In order to do so, the solution of the system must be known in Newtonian sense. In this paper, the Newtonian solution of the bounded system of N equal-mass distinguishable hard particles will be studied with the hope that the time evolution of a given initial distribution function can be calculated explicitly in the near future.

The boundary effects due to walls have been treated without any approximation by "Mirror-Image" transformation. Therefore, we first of all clarify the idea of "Mirror-Image" method, step by step, in Section 2. In Section 3, we show that the motion is equivalent to a straight line in N -dimensional torus with suitable coordinate system and we obtain an algorithm from which the positions and the velocities of N equal-mass distinguishable hard particles can be determined from their initial values. For $N=2$ case, the possible ordering of different collisions of an arbitrary trajectory is analyzed, both qualitatively and quantitatively, in Section 4. Finally, with the help of results in the previous sections, we are able to derive the equilibrium distribution function and to calculate some statistical quantities in Section 5.

2. THE MIRROR-IMAGE TRANSFORMATION

In thermodynamics, we usually deal with the systems having definite boundaries (including impenetrable walls). One often neglects the wall forces, either by assuming that the system has infinite extent, or by assuming the so-called periodic boundary conditions². The periodic boundary conditions may be regarded as an approximate way of dealing with the boundary effects, valid for the large systems (for which the boundary effects are likely to be unimportant anyway). However, the boundary effects do play an important role for the systems with only a few particles, and hence these effects cannot be neglected.

The periodic boundary conditions introduced by Born³ can take care of the hard wall potentials completely (with no approximation). We clarify this by considering the simplest conceivable bounded system:

one hard particle in a one-dimensional box of length R . The Hamiltonian is

$$H_1 = \frac{p^2}{2m} + V_W(q) \quad 0 \leq q \leq \ell, \quad (1)$$

where the wall potential $V_W(q)$ is infinite when $q = 0$ or R and zero otherwise. From Newton's first law, this hard particle will move linearly with constant velocity until hitting the walls, and then bounce back and forth between the walls. By considering $(q(0), v(0))$ as the initial conditions, the motion can be represented by the zig-zag line $X_0 P(X_0 = q(0))$, with alternating slopes $\pm v(0)$, as shown in Figure 1.

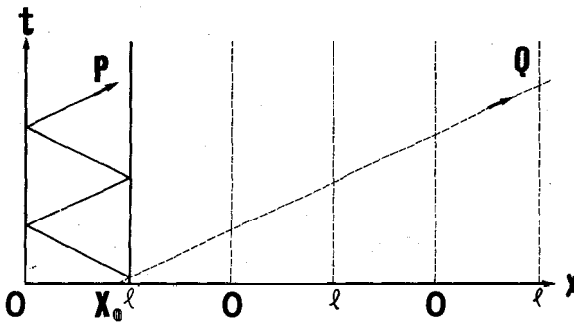


Fig.1 - The zig-zag motion $X_0 P$ of one hard particle in a one-dimensional box of length ℓ and its image $X_0 Q$ in a one-dimensional torus of length 2ℓ , with the coordinate from zero through R than back to 0.

The basic idea of Born is that we can obtain exactly the same motion by imagining that whenever the hard particle hits the wall, it simply passes through the wall and at the same time, another hard particle enters the wall with the same velocity but in the opposite direction. This can be achieved by replacing the hard particle with the initial conditions $(q(0), v(0))$ by an infinite set of freely moving hard particles with the initial conditions $(q_n(0), v_n(0))$. The following relations (for the detail, see Born³)

$$\begin{aligned} q_{2n}(0) &= 2n\ell + q(0), & v_{2n}(0) &= v(0); \\ q_{2n+1}(0) &= 2n\ell - q(0), & v_{2n+1}(0) &= -v(0), \end{aligned} \quad (2)$$

n being any integer, must be satisfied. Here we have assumed that the 0 -th particle is the original particle or $q_0(0) = q(0)$ and $v_0(0) = v(0)$. The above relations can easily be obtained directly by considering the walls just as perfect reflecting mirrors and by collecting all the images of the point $(q(0), v(0))$. In doing so, the Hamiltonian (1) becomes

$$\bar{H}_1 = \sum_{n=-\infty}^{\infty} \frac{p_n^2}{2m} \quad (-\infty < q_n < \infty) \quad (3)$$

and the initial conditions of hard particles are $(q_n(0), v_n(0))$. Thus the wall potentials have been removed completely.

For later convenience, we consider the walls as perfect mirrors which reflect the coordinate system, instead of the point $(q(0), v(0))$ as Born does. The configurations space then becomes a one-dimensional torus of length 2ℓ with the coordinate system, from the origin through ℓ than back to the origin (or 2ℓ), as shown in Figure 1. Now we define the "Mirror-Image" transformation as

$$|x| = s(x)\ell + r(x) \quad -\infty < x < \infty \quad (4)$$

where $s(x)$ is zero or positive integer and $0 \leq r(x) \leq \ell$,

$$q = r(x) \quad \text{for } s(x) \text{ being even,} \quad (5)$$

and

$$q = R - r(x) \quad \text{for } s(x) \text{ being odd.}$$

The Hamiltonian (1) then becomes after the above "Mirror-Image" transformation

$$H_1 = \frac{p^2}{2m} \quad (6)$$

with the initial conditions $(q(0), v(0))$. Hence the motion is a straight line X_0Q as shown in Figure 1. More explicitly, by substituting the displacement $x(t) = q(0) + v(0)t$ of the hard particle for x in Equation (4), the Newtonian solution can be written as

$$q(t) = r(x(t)) \quad v(t) = \pm v(0) ,$$

and

$$q(t) = \ell - r(x(t)) \quad v(t) = \mp v(0)$$

for $s(x(t))$ being even and odd, respectively. The upper and lower signs are valid respectively for $x(t) \geq 0$ and $x(t) < 0$.

Let us now consider the bounded system of N equal-mass indistinguishable (non-interacting) hard particles. We suppose that the Hamiltonian is

$$H_{I,N} = \sum_{i=1}^N \left\{ \frac{p_i^2}{2m} + V_W(q_i) \right\} \quad 0 \leq q_i \leq \ell \quad (8)$$

and that the initial conditions of the hard particles are $(q_i(0), v_i(0))$. This system has been studied by hobson and Loomis⁴ and Cheng⁵ by using Born's periodic conditions. Now, we put the above "Mirror-Image" transformation into more general form:

$$|x_i| = s(x_i)\ell + r(x_i) \quad -\alpha < x_i < \alpha , \quad (9)$$

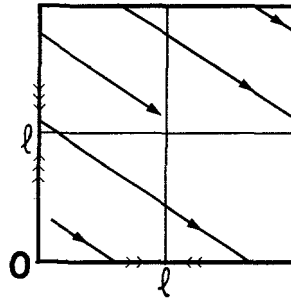
where $s(x_i)$ is zero or positive integer and $0 \leq r(x_i) \leq R$,

$$\begin{aligned} q_i &= r(x_i) && \text{for } s(x_i) \text{ being even,} \\ q_i &= \ell - r(x_i) && \text{for } s(x_i) \text{ being odd} \end{aligned} \quad (10)$$

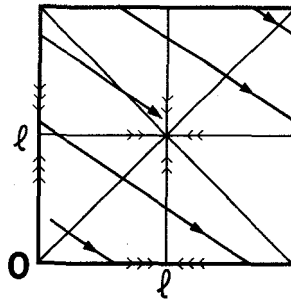
for each hard particle. After this "Mirror-Image" transformation, the Hamiltonian (8) becomes

$$H_{I,N} = \sum_{i=1}^N \frac{p_i^2}{2m} \quad (11)$$

Therefore, the motion is a straight line in a N -dimensional torus with the coordinate from the origin through R then back to the origin (or 2ℓ) for each dimension. For the case $N=2$, a typical trajectory is shown in Figure 2(a). Furthermore, by substituting the displacement $x_i(t) = q_i(0) + v_i(0)t$ of each hard particle for x_i in Equation (9), the Newtonian solution can be put into the following forms:



(a)



(b)

Fig.2 - (a) A typical trajectory of two indistinguishable and (b) of two distinguishable hard particles in a two-dimensional torus with \rightarrow and $\rightarrow\rightarrow$ stand for the coordinate axes of two hard particles.

$$q_i(t) = r(x_i(t)) \quad v_i(t) = \pm v_i(0) , \tag{12}$$

$$q_i(t) = l - r(x_i(t)) \quad v_i(t) = \mp v_i(0)$$

for $s(x_i(t))$ being even and odd, respectively. Here the upper and lower signs are respectively for $x_i(t) \geq 0$ and $x_i(t) < 0$. In the next section we will use Equations (9), (10) and (12) for the bounded system of N equal-mass distinguishable hard particles.

3. THE NEWTONIAN SOLUTION

For the bounded system of N equal-mass distinguishable hard particles in a one-dimensional box of length R, the Hamiltonian is in the following form*

$$H_{D,N} = \sum_{i=1}^N \left\{ \frac{p_i^2}{m} + V_W(q_i) \right\} + \sum_{i,j=1}^N V_H(q_i, q_j) , \quad (13)$$

where the hard pair potential $V_H(q_i, q_j)$ is infinite for $q_i > q_j$ ($i < j$) and zero otherwise, and $V_W(q_i)$ is the wall potential. Here we have assumed that the hard particles are distinguishable and have assigned each hard particle a positive integer (1 through N) according to its initial position $q_i(0)$; $i < j$ if and only if $q_i(0) < q_j(0)$. The hard pair potential $V_H(q_i, q_j)$ will keep this ordering (distinguishability) for all time t , or

$$q_i(t) < q_j(t) \text{ if and only if } q_i(0) < q_j(0) . \quad (14)$$

After the "Mirror-Image" transformations (9) and (10), the Hamiltonian (13) then becomes

$$H_{D,N} = \sum_{i=1}^N \frac{p_i^2}{2m} + \sum_{i,j=1}^N V_H(q_i, q_j) . \quad (15)$$

Therefore, the wall potentials have been removed completely as we did before for the bounded system of N equal-mass indistinguishable hard particles. From now on we only have to study the effects of the hard potential $V_H(q_i, q_j)$ or the collisions among the hard particles.

It is well known that when two equal-mass hard particles collide, the hard pair potential $V_H(q_i, q_j)$ can only exchange their velocities. Therefore, their motion will be straight lines by exchange their assigned numbers right after the collision. In other words, we have

$$q_i^{\dagger} = q_j \text{ and } q_j^{\dagger} = q_i , \quad (16)$$

where \dagger stands for the coordinate right after the collision. For later calculations we achieve the same goal by exchanging their coordinate axes: We actually divide the configuration space (N -dimensional torus having the coordinate from 0 through R than back to 0 for each dimension) into $2^N(N!)$ regions (see next section) by the collision surface $S_N = \{(q_1, q_2, \dots, q_N) \mid \text{at least two of } q_i \text{ are equal or at least one of } q_i \text{ is zero or } R \text{ (} i = 1, 2, \dots, N)\}$. Actually, each region represents

a momentum state. Now, it can easily be seen that the motion of our system is a straight line in the configuration space mentioned above. For the case $N = 2$, a typical trajectory is shown in Figure 2(b).

With the help of the previous results, we are able to obtain the Newtonian solution; the dynamic state of the system can be predicted from its initial state. More explicitly, giving their initial values, the positions and momenta of N equal-mass distinguishable hard particles for any time t can be determined by the following algorithm;

(1) calculate the displacement, $x_i(t) = q_i(0) + v_i(0)t$, for each hard particle,

(2) calculate the position $q_i(t)$ and the velocity $v_i(t)$ by using Equation (12) for each hard particle,

(3) rearrange $q_i(t)$ ($i = 1, 2, \dots, N$) in the increasing order and reassign a new integer i' (1 through N) according to this new ordering (due to distinguishability),

(4) write down the position $q_{i'}(t)$ and the velocity $v_{i'}(t)$ for each hard particle.

In principle, we solve the problem for any integer N . From practice point of view, the above calculations can be carried out without much difficulties for quite large integer N , by using the modern electronic computer.

4. ANALYSIS OF COLLISIONS FOR $N = 2$

It is well known that there exists another integral of motion

$$I_N = \sum_{i,j=1}^N \left| \frac{p_i}{p_j} \right| \quad (i \neq j) \quad (17)$$

besides the energy

$$E_N = \sum_{i=1}^N \frac{p_i^2}{2m} \quad (18)$$

for Hamiltonian system (13). Equation (18) represents a $(N-1)$ -dimensional surface of a N -dimensional sphere of radius $\sqrt{2mE_N}$. It can easily be shown that the intersection $I_N \cap E_N$, at most contains $2^N(N!)$ points

in the surface E_N . In other words, there are at most $2^N(N!)$ allowed momentum states (depending on the initial momentum state). As we already know, the configurations space becomes

$$C_N = \{(q_1, q_2, \dots, q_N) \mid 0 \leq q_1 \leq \dots \leq q_N \leq \ell\} \quad (19)$$

due to the hard pair potential $V_H(q_i, q_j)$. Therefore the motion should be restricted to the reduced phase space, $P_N = C_N \otimes (I_N \cap E_N)$. More explicitly, the motion is a straight line in the reduced phase space P_N .

For the case $N=2$, the intersection $I_2 \cap E_2$ consists of eight points ($v_1(0) \neq v_2(0)$ are assumed), labeled from 1 through 8 in E_2 as shown in Figure 3. Thus the reduced phase space P_2 can be represented by Figure 4, in which the integer assigned to the region corresponds to the same momentum state as in Figure 3. The arrows \longrightarrow and $\longrightarrow\longrightarrow$ stand for coordinate axes of q_1 and q_2 , respectively. The trajectory is a straight line in P_2 and its inclination depends on the ratio of $v_1(0)$ and $v_2(0)$.

For later convenience we classify the different collisions by its momentum states before and after the collision. Thus the collision $C_{i \rightarrow j}$ ($i, j = 1, 2, \dots, 8$) stands for the collision with the momentum states i (before collision) and j (after collision). Let us restrict the initial momentum state to be state 1; $p_1(0) \geq 0$ (or $v_1(0) \geq 0$), $p_2(0) \leq 0$ (or $v_2(0) \leq 0$) and $|p_2(0)/p_1(0)| \leq 1$. To do this we note that we only con-

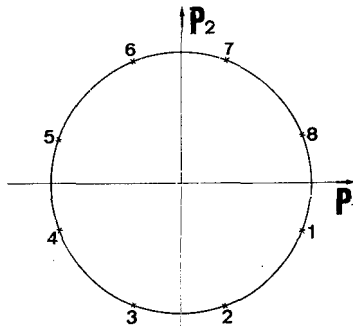


Fig.3 - The energy surface I , in the momentum space and the possible momentum states in a single trajectory.

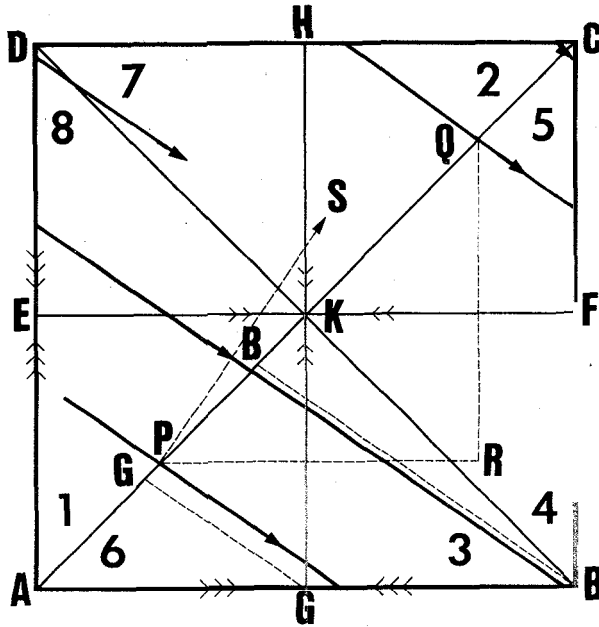


Fig.4 - A typical trajectory with the initial momentum state 1 ($-\pi/4 < \phi < 0$) in the reduced phase space P_2 .

consider the trajectories with the inclination ϕ such as $-\pi/4 \leq \phi \leq 0$ (in the region 1), which implies that only some of the collisions C_{i-j} can happen.

Since the trajectory is a straight line as shown in Figure 4, we have no difficulty to determine the collision C_{i-j} whenever the trajectory hits the collision lines (AB, AC, BC, BD, EF and GH) and the collision vertices (B, F, G and K). For instance, as the trajectory hits the vertex F (or G), it means that the first hard particle collides with the left wall when the second hard particle collides with the right wall. The momentum (or velocity) of each hard particle is reversed right after the collision. Hence the collision at vertex F and G is respectively C_{5-1} and C_{6-2} . In similar arguments, we can show that the collision at vertex B and K is C_{3-7} and C_{8-4} , respectively.

After careful analysis, the possible collisions and their orders in a trajectory are shown in Figure 5. There exist only sixteen different collisions, which in turn make ten groups of collisions;

$$\begin{aligned}
G_0 &= C_{1-6}C_{6-2}, & G_5 &= C_{2-5}C_{5-1}, \\
G_1 &= C_{1-6}C_{6-7}C_{7-2}, & G_6 &= C_{2-5}C_{5-4}C_{4-1}, \\
G_2 &= C_{1-6}C_{6-3}C_{3-2}, & G_7 &= C_{2-5}C_{5-8}C_{8-1}, \\
G_3 &= C_{1-6}C_{6-3}C_{3-7}C_{7-2}, & G_8 &= C_{2-5}C_{5-8}C_{8-4}C_{4-1}, \\
G_4 &= C_{2-5}C_{5-8}C_{8-7}C_{7-2}, & G_9 &= C_{1-6}C_{6-3}C_{3-4}C_{4-1}.
\end{aligned} \tag{20}$$

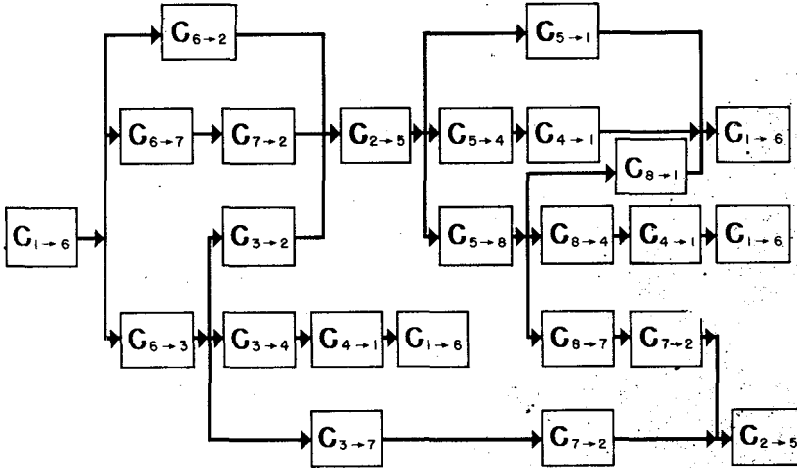


Fig.5 - The possible collisions and their orders in a single trajectory.

For the trajectory with the initial momentum state other than 1, we only have to wait a finite time until it reaches the momentum state 1 and apply the above results. Therefore, the trajectory can be represented by a sequence of G_0, G_1, \dots, G_9 which satisfies the following rules;

- (1) G_0, G_1, G_2, G_3 and G_4 can be followed by G_4, G_5, G_6, G_7 and G_8 , and
- (2) G_5, G_6, G_7, G_8 and G_9 can be followed by G_0, G_1, G_2, G_3 and G_9 .

According to the Jacobi's theorem⁶, the motions are periodic of period $T = 2n\lambda/v_1(0)$ if and only if

$$\frac{v_1(0)}{v_2(0)} = \frac{n}{m} \tag{21}$$

is rational, otherwise, the motions are ergodic. If the motion is ergodic, then the trajectories are dense everywhere in the reduced phase space P_2 and can pass through the vertices B, F, G and K only once for all time t ; the corresponding groups of collisions G_3, G_5, G_0 and G_8 can appear at most once. The conditions for the above mentioned vertex-passing motions are respectively

$$\frac{v_1(0)}{v_2(0)} = \frac{q_1(0) - 2(n+1)\ell}{q_2(0) + 2m\ell}, \quad \frac{v_1(0)}{v_2(0)} = \frac{q_1(0) - 2(n+1)\ell}{q_2(0) + (2m+1)\ell}, \quad (22)$$

$$\frac{v_1(0)}{v_2(0)} = \frac{q_1(0) - (2n+1)\ell}{q_2(0) + 2m\ell}, \quad \frac{v_1(0)}{v_2(0)} = \frac{q_1(0) - (2n+1)\ell}{q_2(0) + (2m+1)\ell}$$

for some integers n and m . Since the initial positions and momenta satisfied Eqs. (21) and (22) are of measure zero, almost all trajectory then can be represented by a sequence of $G_1, G_2, G_4, G_6, G_7, G_9$ which satisfies the following rules;

- (1) G_1, G_2 and G_4 can be followed by G_4, G_6 and G_7 , and G_6, G_7 and G_9 can be followed by G_1, G_2 and G_9 . (2)

In order to obtain Newtonian solution, we also need to know the dates of all possible collisions. For later calculations, we now classify the different collisions in classes by their collision lines, i.e.

$$\begin{aligned} C_{AB} &= \{C_{6-7}, C_{3-2}\}, & C_{AC} &= \{C_{1-6}, C_{2-5}\}, \\ C_{BC} &= \{C_{4-1}, C_{5-8}\}, & C_{BD} &= \{C_{3-4}, C_{8-7}\}, \\ C_{EF} &= \{C_{5-4}, C_{8-1}\}, & C_{GH} &= \{C_{6-3}, C_{7-2}\}. \end{aligned} \quad (23)$$

We may consider that each collision line is a set of parallel lines and the trajectory is a straight line in the reduced phase space P_2 . Therefore, two nearest collision points on each collision line are separated by equal distance and equal time intervals. In other words, on the one hand, the motion is equivalent to a rotation along each collision line,

while on the other hand, the time interval between two nearest collisions of the same class is constant. Moreover, we have:

Theorem 1: The time interval between two nearest collisions of the same class is equal to (a) $\Delta t_{AC} = 2\ell / (v_{1,0} - v_{2,0})$, (b) $\Delta t_{BD} = 2\ell / (v_{1,0} + v_{2,0})$, (c) $\Delta t_{BC} = \Delta t_{GH} = 2\ell / v_{1,0}$ and (d) $\Delta t_{AB} = \Delta t_{EF} = -2\ell / v_{2,0}$ ($v_{1,0} = v_1(0)$ and $v_{2,0} = v_2(0)$).

Proof: It is evident from Figure 4 that the time interval between two nearest collisions of C_{BC} (or C_{GH}) and of C_{AB} (or C_{EF}) are respectively equal to the time it takes for the trajectory in moving through distance 2ℓ horizontally and vertically. We obtain the results (c) and (d) since the trajectory moves with the velocity $v_{1,0}$ ($-v_{2,0}$) horizontally (vertically). For two nearest collisions of C_{AC} , we assume P and Q to be the corresponding collision points. Drawing the lines $\overline{PR} // \overline{EF}$ and $\overline{QR} // \overline{GH}$, we then have $\overline{PR} = \overline{QR}$. The trajectory moves through \overline{PR} horizontally (to the right) and $2\ell - \overline{QR}$ vertically (downward) during the time interval Δt_{AC} , or $v_{1,0} \Delta t_{AC} = \overline{PR}$ and $v_{2,0} \Delta t_{AC} = 2\ell - \overline{QR}$. We obtain (a) by eliminating \overline{PR} and \overline{QR} . Since $AC \perp BD$, we can obtain (b) by rotating the trajectory 90 degrees to the line PS and by applying the same arguments as we did for obtaining (a).

Now, we consider the collision line AC as the surface of section⁷ and investigate the motion of the points on it. We then have:

Corollary: The motion is a rotation with angular velocity

$$\theta = \sqrt{2}\pi \left\{ 1 + \frac{2v_{2,0}}{v_{1,0} - v_{2,0}} + \frac{v_{1,0}^2 + v_{2,0}^2}{(v_{1,0} - v_{2,0})^2} \right\}^{1/2} \quad (24)$$

around the circle AC.

Proof: From Theorem 1, the distance between P and Q can be written as

$$\overline{PQ} = (\overline{PR}^2 + \overline{QR}^2)^{1/2}$$

$$= 2 \left\{ 1 + \frac{2v_{2,0}}{v_{1,0} - v_{2,0}} + \frac{v_{1,0}^2 + v_{2,0}^2}{(v_{1,0} - v_{2,0})^2} \right\} \quad (25)$$

Therefore, Equation (24) has been proved since the circumference of the circle \mathcal{AC} is $2\sqrt{2}l$ (2π degrees).

The trajectory is dense everywhere on the circle \mathcal{AC} if and only if the ratio of 0 and 2π is irrational. From Equation (24), it is obvious that this depends on the ratio of $v_{1,0}$ and $v_{2,0}$. Being irrational or not as we expect.

Theorem 2. If the motion is ergodic, then the probabilities of appearing G_i ($i = 1, 2, 4, 6, 7, 9$) along the trajectory are

$$(a) P(G_1) = P(G_2) = P(G_6) = P(G_7) = \frac{v_{2,0}}{2(v_{1,0} - v_{2,0})}$$

and

(26)

$$(b) P(G_4) = P(G_9) = \frac{v_{1,0} + v_{2,0}}{2(v_{1,0} - v_{2,0})}$$

Proof: Let us draw the lines BB' and GG' , which are parallel to the trajectory. From Equations (20) we see that which one of G_1 , G_2 and G_9 will appear depends only on the collision point along AK as shown in Figure 4. For instance, G_1 will appear if the trajectory passes through the points between the vertices A and G' . Since the trajectory is dense everywhere along the circle \mathcal{AC} , the time average is equal to the ensemble average. In other words, the probabilities of G_1 , G_2 and G_9 depend on $\overline{AG'}$, $\overline{G'B'}$ and $\overline{B'K}$. Since $AAGG' \cong AABB'$, we get $\overline{AB}/\overline{AG'} = \overline{AB'}/\overline{AG'}$ and $\overline{AG'} = \overline{G'B'}$ or $P(G_1) = P(G_2)$. From one of Equations (22) (corresponding to the vertex G), we obtain $q_1(0) = q_2(0) = -v_{2,0}/(v_{1,0} - v_{2,0})$ ($n = 1$ and $m = 0$) and $\overline{AG'} = \sqrt{2} q_1(0)$. We then have $\overline{B'K} = \sqrt{2}l - (\overline{AG'} + \overline{G'B'}) = \sqrt{2}l (v_{1,0} + v_{2,0})/(v_{1,0} - v_{2,0})$. It can easily be seen that C_{3-4} and C_{8-7} should appear with exactly the same probability, or $P(G_4) = P(G_9)$. With similar

arguments, we can show that $P(G_1) = P(G_6) = P(G_7)$. Finally, we obtain the results (a) and (b) by using the normalization condition of $P(G_1)$.

In principle, the Newtonian solution can be determined by calculating the first date of the collision of each class and by dividing from that point the time axis with the time interval of two nearest collision of that class as unit. However, we are not going to discuss this method here in detail. We prefer the method mentioned in Section 3.

5. EQUILIBRIUM PROPERTIES

Since the trajectory is a straight line in the reduced phase space P_N , we are able to show the the motions of N equal-mass distinguishable hard particles in a one-dimensional box of length ℓ are ergodic if and only if

$$\vec{v} \cdot \vec{k} = 0 \quad \text{imply} \quad \vec{k} = 0 \quad (27)$$

where $\vec{v} = (v_1(0), v_2(0), \dots, v_N(0))$ and $\vec{k} = (k_1, k_2, \dots, k_N)$ (k_i being integers) from the Jacob's theorem. Therefore, our dynamic system is ergodic but not mixing.

As we know that the time average is equal to the ensemble average for any ergodic system, we can easily show that the N -body equilibrium position distribution function is

$$Q(q_1, q_2, \dots, q_N, t) \xrightarrow[t \rightarrow \infty]{} \frac{N!}{\ell^N}, \quad (28)$$

here and for later calculations the restrictions $0 \leq q_1 \leq q_2 \leq q_N \leq \ell$ have been used. We then can obtain

$$\begin{aligned} \langle q_k \rangle &= \frac{N!}{\ell^N} \int_0^\ell dq_N \int_0^{q_N} dq_{N-1} \dots \int_0^{q_{k+1}} q_k dq_k \int_0^{q_k} dq_{k-1} \dots \int_0^{q_2} dq_1 \\ &= \frac{k\ell}{N+1}, \end{aligned} \quad (29)$$

$$\begin{aligned}
 \langle q_k q_m \rangle &= \frac{N!}{l^N} \int_0^l dq_N \dots \int_0^{q_{m+1}} q_m dq_m \dots \int_0^{q_k} q_k dq_k \dots \int_0^{q_2} dq_1 \\
 &= \frac{k(m+1) l^2}{(N+1)(N+2)} \quad (m \geq k)
 \end{aligned} \tag{30}$$

and

$$\langle q_k q_m \rangle - \langle q_k \rangle \langle q_m \rangle = \frac{k(N-m+1) l^2}{(N+1)^2 (N+2)} \tag{31}$$

As $N \rightarrow \infty$, we have $\langle q_k q_m \rangle = \langle q_k \rangle \langle q_m \rangle$ for any k and m , thus the positions of any two hard particles are statistically independent (or uncorrelated) as we expect. If the initial velocity distribution function is in the Gauss form

$$P(v_1, v_2, \dots, v_N, 0) = \left[\frac{1}{\sqrt{2\pi}\sigma} \right]^N \prod_{i=1}^N e^{-\frac{(v_i - \bar{v}_i)^2}{2\sigma^2}} \tag{32}$$

where \bar{v}_i and σ are respectively the average velocity and its standard deviation of i -th hard particle. The equilibrium velocity distribution function then becomes

$$\begin{aligned}
 P(|v_1|, |v_2|, \dots, |v_N|, t) &\xrightarrow{t \rightarrow \infty} \left[\frac{1}{2\sqrt{(2\pi)\sigma}} \right]^N \\
 &\prod_{i,j=1}^N \left\{ e^{-\frac{(v_i - \bar{v}_j)^2}{2\sigma^2}} + e^{-\frac{(v_i + \bar{v}_j)^2}{2\sigma^2}} \right\}
 \end{aligned} \tag{33}$$

for the hard pair potential $V_H(q_i, q_j)$ can only exchange the velocities among the hard particles. Equation (33) means Gauss distribution with the mean velocities $\pm \bar{v}_j$, but not a Maxwell distribution. Hence the potentials $V_H(q_i, q_j)$ and $V_W(q_i)$ are not enough to obtain the equilibrium distribution function of an ideal gas. Works are in progress for the time evolution of the distribution function.

REFERENCES

1. I.E. Farquhar, *Ergodic Theory in Statistical Mechanics*, New York, John Wiley & Sons Ltd., 1964.
2. B.J. Alder and J.E. Wainwright, *J. of Chem. Phys.*, 31, 459 (1957).
3. M. Born, *Kgl. Danske. Videnskab. Mat. Fys. Medd.* 30, 1 (1955).
4. A. Hobson and J.E. Loomis, *Phys. Rev.*, 173, 285 (1968).
5. B.K. Cheng, Ph. D. Thesis, University of Arkansas (1974).
6. V.I. Arnold and A. Avez, *Ergodic Problems of Classical Mechanics*, New York, W.A. Benjamin, Inc., 1968.
7. H. Poincaré, *Les Methodes Nouvelles de la Mécanique Céleste*. 3 Vols., New York, Dover Publications, 1957.